New $[Pt_3(\mu_3\text{-}CO)(\mu\text{-}Ph_2PCH_2PPh_2)_3L]^{2+}$ Clusters, L = Phosphine or Phosphite Ligand, Containing an Asymmetric $Pt_3(\mu_3\text{-}CO)$ Group and the Crystal Structure of the Complex with L = $P(OPh)_3$

Arleen M. Bradford,[1a] Graeme Douglas,[1b] Ljubica Manojlović-Muir,*[,1b] Kenneth W. Muir,[1b] and Richard J. Puddephatt*[,1a]

Department of Chemistry, University of Western Ontario, London, Ontario, Canada N6A 5B7, and Chemistry Department, University of Glasgow, Glasgow G12 8QQ, Scotland

Received July 6, 1989

The complex $[Pt_3(\mu_3\text{-}CO)(\mu\text{-}dppm)_3]^{2+}$ (1; dppm = $Ph_2PCH_2PPh_2$) adds phosphorus donors L to give the adducts $[Pt_3(\mu_3\text{-}CO)(\mu\text{-}dppm)_3L]^{2+}$ (2), where L = $P(OMe)_3$ (**2a**), $P(OEt)_3$ (**2b**), $P(OPh)_3$ (**2c**), PMe_2Ph (**2d**), $PMePh_2$ (**2e**), PPh_3 (**2f**), PF_3 (**2g**). Complexes **2a–d** are thermally stable, but **2e–g** readily dissociate the phosphorus donor ligand to regenerate 1. Complex **2c** has been characterized crystallographically. The phosphite ligand binds as a terminal ligand to a single platinum center, and the triply bridging carbonyl ligand is bound most strongly to the same platinum atom. The same structure is believed to be present in solutions of **2a–f** at low temperature, but the complexes **2a–e** exhibit a new type of fluxionality at higher temperatures in which the phosphorus donor ligand migrates around the Pt_3 triangle. The "time-averaged" structure therefore appears to have a μ_3-PX_3 ligand. For complex **2g**, the fluxional process was not frozen out at −90 °C and it is possible that the $Pt_3(\mu_3\text{-}PF_3)$ group is present in the ground state.

Introduction

The complex $[Pt_3(\mu_3\text{-}CO)(\mu\text{-}dppm)_3]^{2+}$ (1; dppm = $Ph_2PCH_2PPh_2$)[2] has the typical 42-electron count of Pt_3 clusters,[3] and hence, each platinum atom is coordinatively unsaturated. Since the μ-dppm ligands prevent easy fragmentation of the cluster, complex **1** has proved to be a useful model for reactions at a 3-fold site of a Pt(111) surface.[4,5] The simplest surface reaction that can be mimicked by a coordinatively unsaturated cluster is nondissociative chemisorption.[6] In the terminology of coordination chemisty, this is just ligand addition or complex formation and this paper reports the addition of tertiary phosphine and phosphite ligands to complex **1**. The interest is in whether the ligands add at terminal or bridging sites,[5,7-11] in how ligand addition affects the $Pt_3(\mu^3\text{-}CO)$ linkage,[10,11] and in whether the added ligand or carbonyl ligand is fluxional.[5,7,8,10] It has been shown previously that some phosphine ligands, L, add reversibly to the 42-electron clusters $[Pt_3(\mu\text{-}CO)_3L_3]$ to give $[Pt_3(\mu\text{-}CO)_3L_4]$, and this can lead to ligand substitution reactions or, especially with less bulky ligands L, to cluster fragmentation.[3,12] It is recognized that phosphine and, to a lesser extent, phosphite ligands are of major importance in cluster chemistry,[13] and with respect to the surface analogy, it is believed that PH_3 and PF_3 add as terminal ligands on the Pt(111) or Ni(111) surface.[14]

A preliminary account of parts of this work has been published.[15]

Results

Formation of the Complexes $[Pt_3(\mu_3\text{-}CO)(\mu\text{-dppm})_3L][PF_3]_2$. As monitored by ^{31}P NMR spectroscopy, the reaction of $[Pt_3(\mu_3\text{-}CO)(\mu\text{-}dppm)_3]^{2+}$ (1) with the less bulky phosphite and phosphine ligands $P(OMe)_3$, $P(OEt)_3$, $P(OPh)_3$, and PMe_2Ph gave the corresponding complexes **2a–d**, respectively, in essentially quantitative yield. These complexes were thermally stable and could

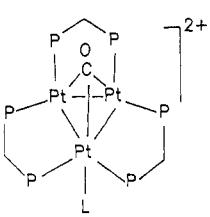

	L
2a	$P(OMe)_3$
2b	$P(OEt)_3$
2c	$P(OPh)_3$
2d	PMe_2Ph
2e	$PMePh_2$
2f	PPh_3
2g	PF_3

be isolated in analytically pure form as the hexafluorophosphate salts, which were red solids. However, with the bulkier ligands $PMePh_2$ and PPh_3, adduct formation was reversible and the adducts **2e** and **2f** could not be isolated in pure form. Similarly, the volatile ligand PF_3 formed the complex **2g**, as determined by NMR spectroscopy, but partial loss of PF_3 occurred on attempted isolation.

For the ligand PPh_3 it was possible to measure the equilibrium constant, K, for formation of **2f** by integration

(1) (a) University of Western Ontario. (b) University of Glasgow.
(2) Ferguson, G.; Lloyd, B. R.; Puddephatt, R. J. *Organometallics* **1986**, *5*, 344.
(3) (a) Mingos, D. M. P.; Wardle, W. M. *Transition Met. Chem.* **1985**, *10*, 441. (b) Eremenko, N. K.; Mednikov, E. G.; Kurasov, S. S. *Russ. Chem. Rev. (Engl. Transl.)* **1985**, *54*, 394.
(4) Jennings, M. C.; Manojlović-Muir, Lj.; Puddephatt, R. J. *J. Am. Chem. Soc.* **1989**, *111*, 745.
(5) Lloyd, B. R.; Bradford, A. M.; Puddephatt, R. J. *Organometallics* **1987**, *6*, 424.
(6) Muetterties, E. L.; Rhodin, T. N.; Band, E.; Brucker, C. F.; Pretzer, W. R. *Chem. Rev.* **1979**, *79*, 91.
(7) Ferguson, G.; Lloyd, B. R.; Manojlović-Muir, Lj.; Muir, K. W.; Puddephatt, R. J. *Inorg. Chem.* **1986**, *25*, 4190.
(8) Jennings, M. C.; Puddephatt, R. J. *Inorg. Chem.* **1988**, *27*, 4280.
(9) Jennings, M. C.; Manojlović-Muir, Lj.; Muir, K. W.; Puddephatt, R. J. *J. Chem. Soc., Chem. Commun.*, in press.
(10) Evans, D. G. *J. Organomet. Chem.* **1988**, *352*, 397.
(11) Mealli, C. J. *Am. Chem. Soc.* **1985**, *107*, 2245.
(12) (a) Chatt, J.; Chini, P. *J. Chem. Soc. A* **1970**, 1538. (b) Browning, C. S.; Farrar, D. H.; Gukathasan, R. R.; Morris, S. A. *Organometallics* **1985**, *4*, 1750. (c) Mingos, D. M. P.; Williams, I. D.; Watson, M. J. *J. Chem. Soc., Dalton Trans.* **1988**, 1509.
(13) Evans, D. G.; Hallam, M. F.; Mingos, D. M. P.; Wardle, R. W. M. *J. Chem. Soc., Dalton Trans.* **1987**, 1889.
(14) Mitchell, G. E.; Henderson, M. A.; White, J. M. *Surf. Sci.* **1987**, *191*, 425. Alvey, M. D.; Yates, J. T., Jr. *J. Am. Chem. Soc.* **1988**, *110*, 1782.
(15) Bradford, A. M.; Jennings, M. C.; Puddephatt, R. J. *Organometallics* **1988**, *7*, 792.
(16) The details of formation of adducts of 1 with isocyanides will be reported elsewhere, since they are complex reactions: Bradford, A. M.; Puddephatt, R. J.; Manojlović-Muir, Lj. Unpublished results.

0276-7333/90/2309-0409$02.50/0

Table I. Selected Bond Lengths and Angles in $[Pt_3(\mu_3\text{-}CO)(\mu\text{-}dppm)_3(P(OPh)_3)]^{2+}$ (2c)

Bond Lengths (Å)			
Pt(1)-Pt(2)	2.656 (2)[a]	Pt(1)-Pt(3)	2.626 (2)
Pt(1)-P(1)	2.341 (8)	Pt(1)-P(6)	2.335 (8)
Pt(1)-P(7)	2.293 (8)	Pt(1)-C(4)	1.93 (3)
Pt(2)-Pt(3)	2.636 (2)	Pt(2)-P(2)	2.323 (8)
Pt(2)-P(3)	2.290 (8)	Pt(2)-C(4)	2.16 (3)
Pt(3)-P(4)	2.288 (8)	Pt(3)-P(5)	2.300 (8)
Pt(3)-C(4)	2.27 (3)	P(1)-C(1)	1.81 (3)
P(1)-C(A1)	1.80 (3)	P(1)-C(B1)	1.83 (3)
P(2)-C(1)	1.88 (3)	P(2)-C(C1)	1.84 (3)
P(2)-C(D1)	1.83 (3)	P(3)-C(2)	1.76 (3)
P(3)-C(E1)	1.85 (3)	P(3)-C(F1)	1.85 (3)
P(4)-C(2)	1.89 (3)	P(4)-C(G1)	1.83 (3)
P(4)-C(H1)	1.81 (3)	P(5)-C(3)	1.83 (3)
P(5)-C(I1)	1.84 (3)	P(5)-C(J1)	1.82 (3)
P(6)-C(3)	1.82 (3)	P(6)-C(K1)	1.83 (4)
P(6)-C(L1)	1.85 (3)	P(7)-O(1)	1.56 (2)
P(7)-O(2)	1.57 (2)	P(7)-O(3)	1.59 (2)
O(1)-C(11)	1.40 (4)	O(2)-C(21)	1.44 (4)
O(3)-C(31)	1.37 (3)	O(4)-C(4)	1.21 (4)
Bond Angles (deg)			
Pt(2)-Pt(1)-Pt(3)	59.9 (1)	Pt(2)-Pt(1)-P(1)	98.2 (2)
Pt(2)-Pt(1)-P(6)	148.8 (2)	Pt(2)-Pt(1)-P(7)	94.2 (2)
Pt(2)-Pt(1)-C(4)	53.4 (8)	Pt(3)-Pt(1)-P(1)	156.9 (2)
Pt(3)-Pt(1)-P(6)	93.2 (2)	Pt(3)-Pt(1)-P(7)	90.5 (2)
Pt(3)-Pt(1)-C(4)	57.4 (8)	P(1)-Pt(1)-P(6)	105.1 (3)
P(1)-Pt(1)-P(7)	99.1 (3)	P(1)-Pt(1)-C(4)	104.7 (9)
P(6)-Pt(1)-P(7)	102.1 (3)	P(6)-Pt(1)-C(4)	100.1 (8)
P(7)-Pt(1)-C(4)	141.8 (8)	Pt(1)-Pt(2)-Pt(3)	59.5 (1)
Pt(1)-Pt(2)-P(2)	95.1 (2)	Pt(1)-Pt(2)-P(3)	153.3 (2)
Pt(1)-Pt(2)-C(4)	45.9 (8)	Pt(3)-Pt(2)-P(2)	154.6 (2)
Pt(3)-Pt(2)-P(3)	93.9 (2)	Pt(3)-Pt(2)-C(4)	55.5 (8)
P(2)-Pt(2)-P(3)	111.5 (3)	P(2)-Pt(2)-C(4)	107.9 (8)
P(3)-Pt(2)-C(4)	122.9 (8)	Pt(1)-Pt(3)-Pt(2)	60.6 (1)
Pt(1)-Pt(3)-P(4)	156.3 (2)	Pt(1)-Pt(3)-P(5)	95.0 (2)
Pt(1)-Pt(3)-C(4)	45.7 (8)	Pt(2)-Pt(3)-P(4)	95.7 (2)
Pt(2)-Pt(3)-P(5)	155.2 (2)	Pt(2)-Pt(3)-C(4)	51.6 (7)
P(4)-Pt(3)-P(5)	108.7 (3)	P(4)-Pt(3)-C(4)	120.3 (7)
P(5)-Pt(3)-C(4)	115.5 (7)	Pt(1)-P(1)-C(1)	106.2 (9)
Pt(1)-P(1)-C(A1)	123.5 (8)	Pt(1)-P(1)-C(B1)	115.7 (10)
C(1)-P(1)-C(A1)	98.4 (12)	Cn1)-P(1)-C(B1)	107.9 (11)
C(A1)-P(1)-C(B1)	103.1 (12)	Pt(2)-P(2)-C(1)	110.0 (8)
Pt(2)-P(2)-C(C1)	124.3 (12)	Pt(2)-P(2)-C(D1)	111.7 (11)
C(1)-P(2)-C(C1)	99.5 (12)	C(1)-P(2)-C(D1)	102.4 (12)
C(C1)-P(2)-C(D1)	106.2 (14)	Pt(2)-P(3)-C(2)	110.4 (9)
Pt(2)-P(3)-C(E1)	118.8 (9)	Pt(2)-P(3)-C(F1)	116.6 (8)
C(2)-P(3)-C(E1)	101.9 (14)	C(2)-P(3)-C(F1)	105.6 (12)
C(E1)-P(3)-C(F1)	101.8 (11)	Pt(3)-P(4)-C(2)	106.1 (9)
Pt(3)-P(4)-C(G1)	116.4 (10)	Pt(3)-P(4)-C(H1)	121.1 (11)
C(2)-P(4)-C(G1)	105.0 (12)	C(2)-P(4)-C(H1)	105.6 (14)
C(G1)-P(4)-C(H1)	101.2 (14)	Pt(3)-P(5)-C(3)	112.2 (9)
Pt(3)-P(5)-C(I1)	113.0 (10)	Pt(3)-P(5)-C(J1)	118.6 (10)
C(3)-P(5)-C(I1)	103.2 (12)	C(3)-P(5)-C(J1)	100.4 (13)
C(I1)-P(5)-C(J1)	107.7 (16)	Pt(1)-P(6)-C(3)	106.6 (9)
Pt(1)-P(6)-C(K1)	117.4 (8)	Pt(1)-P(6)-C(L1)	121.0 (9)
C(3)-P(6)-C(K1)	107.3 (15)	C(3)-P(6)-C(L1)	103.7 (11)
C(K1)-P(6)-C(L1)	99.4 (11)	Pt(1)-P(7)-O(1)	109.8 (8)
Pt(1)-P(7)-O(2)	110.7 (8)	Pt(1)-P(7)-O(3)	124.0 (8)
O(1)-P(7)-O(2)	106.9 (11)	O(1)-P(7)-O(3)	96.9 (11)
O(2)-P(7)-O(3)	106.8 (10)	P(7)-O(1)-C(11)	131.1 (15)
P(7)-O(2)-C(21)	130.1 (20)	P(7)-O(3)-C(31)	131.3 (18)
P(1)-C(1)-P(2)	121.5 (14)	P(3)-C(2)-P(4)	111.6 (13)
P(5)-C(3)-P(6)	114.6 (15)	Pt(1)-C(4)-Pt(2)	80.7 (11)
Pt(1)-C(4)-Pt(3)	76.8 (10)	Pt(1)-C(4)-O(4)	154.6 (21)
Pt(2)-C(4)-Pt(3)	72.9 (8)	Pt(2)-C(4)-O(4)	121.1 (19)
Pt(3)-C(4)-O(4)	119.9 (20)		

[a] Estimated standard deviations in the least significant digit are shown in parentheses, here and throughout the paper.

of ^{31}P NMR resonances due to free reagents and complex **2f** over the narrow temperature region −83 to −92 °C. At higher temperatures, exchange broadening was severe and the equilibrium was unfavorable, and −92 °C was the lower limit of temperature that could be studied in acetone-d_6. The approximate thermodynamic parameters were $\Delta H°$ = −42 ± 10 kJ mol^{-1} and $\Delta S°$ = −200 ± 40 J K^{-1} mol^{-1}. Thus, as expected, the enthalpy term favors complex formation but the entropy term does not.

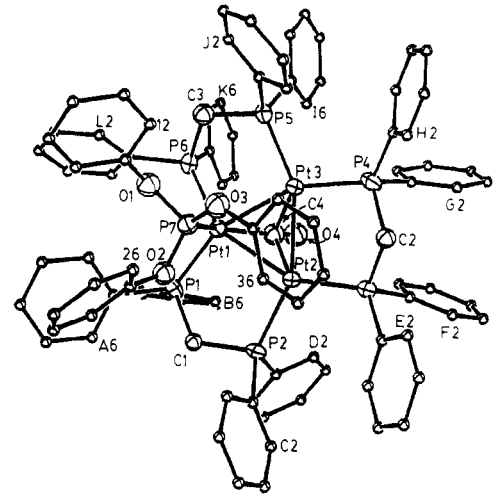

Figure 1. Structure of $[Pt_3(\mu_3\text{-}CO)(\mu\text{-}dppm)_3(P(OPh)_3)]^{2+}$ (**2c**), showing the atomic labeling scheme. In the phenyl rings, carbon atoms are numbered cyclically, C(n1)–C(n6), with n = 1–3, A–L and C(n1) bonded to phosphorus. For clarity, only the C(n2) or C(n6) atoms are labeled by n2 or n6.

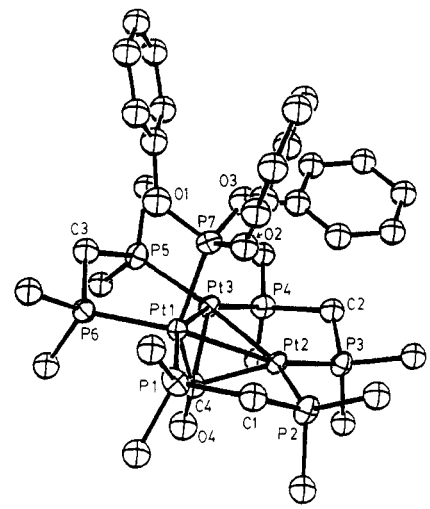

Figure 2. Another view of the structure of **2c**, illustrating the geometry of the $Pt_3(\mu_3\text{-}CO)(P(OPh)_3)$ unit and conformations of the three Pt_2P_2C rings. In the dppm ligands, all but the α-carbons of the phenyl rings are omitted for clarity.

The ^{31}P NMR experiment showed that exchange between free and coordinated PPh_3 occurred rapidly at room temperature, but similar exchange between free and coordinated $P(OMe)_3$ in **2a** did not occur rapidly on the NMR time scale at temperatures up to 100 °C. The ligand exchange with PPh_3 therefore almost certainly occurs by a dissociative mechanism. Exchange could occur with the smaller ligands, but at a much slower rate.

Structure of $[Pt_3(\mu_3\text{-}CO)(\mu\text{-}dppm)_3(P(OPh)_3)][PF_6]_2$ (2c[PF$_6$]$_2$). The crystals of **2c**[PF$_6$]$_2$, whose structure was determined by X-ray diffraction, were grown from an acetone solution, and they are built of well-separated cations, anions, and solvent molecules. The last species were revealed only partially by electron density maps, and their identity and the stoichiometric coefficient in the formula of the compound could therefore not be established.

The structure of the cation (Figure 1) is characterized by bond lengths and angles shown in Table I. It contains

Table II. Comparison of Selected Structural and Spectroscopic Data for $Pt_3(\mu_3\text{-}CO)$ Complexes

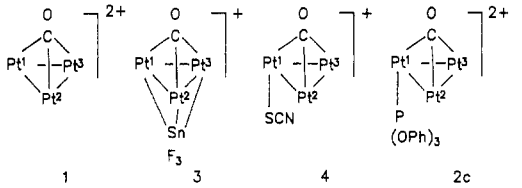

1 3 4 2c

	1[2]	3[9,a]	4[7]	2c
Pt^1–Pt^2/Å	2.638 (1)	2.639 (3)	2.620 (1)	2.656 (2)
Pt^1–Pt^3/Å	2.650 (1)		2.625 (1)	2.626 (2)
Pt^2–Pt^3/Å	2.613 (1)		2.623 (1)	2.636 (2)
Pt^1–C/Å	2.095 (9)	2.16 (5)	2.042 (13)	1.93 (3)
Pt^2–C/Å	2.089 (8)		2.165 (13)	2.16 (3)
Pt^3–C/Å	2.080 (9)		2.175 (13)	2.27 (3)
Pt^1–C–O/deg	131.8 (6)	135 (2)	143.8 (11)	154.6 (21)
Pt^2–C–O/deg	133.1 (7)		129.8 (10)	121.1 (14)
Pt^3–C–O/deg	134.9 (7)		128.9 (10)	119.9 (20)
ν(CO)/cm^{-1}	1765	1827	1810	1779
$^1J(PtC)^b$/Hz	770	650	868	630
$^1J(Pt^1C)$/Hz	...	...	...	960
$^1J(Pt^2C)^c$/Hz	...	...	...	493
$\delta(^{13}CO)$/ppm	205	198	198	194

[a] This complex has crystallographically imposed 3-fold symmetry. [b] For 4 and 2c, this is the average value in the fast-fluxionality region. [c] $^1J(Pt^2C) = {}^1J(Pt^3C)$ in all cases.

an approximately equilateral triangular Pt_3 cluster, with each edge of the triangle bridged by a dppm ligand to form a Pt_2P_2C dimetallacycle. Rotational orientation of the dppm ligands about the Pt–Pt bonds and conformations of the Pt_2P_2C rings are such as to afford a Pt_3P_6 skeleton substantially distorted from an idealized latitudinal M_3L_6 geometry. The largest distortions involve the phosphorus atoms coordinated to the platinum center to which the $P(OPh)_3$ ligand is also bound (Pt(1)). Thus, the P(1) and P(6) atoms lie 0.321 (8) and 0.669 (7) Å away from the Pt_3 plane, on the side opposite to that of the $P(OPh)_3$ ligand. In the Pt_2P_2C rings the methylene groups are pointing toward the $P(OPh)_3$ ligand, the atoms C(1), C(2), and C(3) being displaced from the Pt_3 plane by 0.23 (2), 0.81 (3), and 0.21 (3) Å, respectively. In this conformation of the $Pt_3P_6C_3$ skeleton, the phenyl rings are directed away from the bulky $P(OPh)_3$ ligand and the steric hindrance, which is severe, is thus minimized.

The Pt–Pt distances (2.656 (2), 2.636 (2), and 2.626 (2) Å) differ only slightly from each other, and their mean value (2.639 Å) is similar to the mean Pt–Pt distance in complex 1 (2.634 Å).[2] Thus, the addition of the phosphite ligand to 1 increases the cluster electron count from 42e to 44e, but it does not significantly affect the Pt–Pt bond lengths; this is in accord with our recent findings on related complexes.[7,9,17] However, the Pt–P(dppm) bond lengths involving the Pt(1) atom (2.341 (8) and 2.335 (8) Å) are longer than those involving Pt(2) and Pt(3) (2.288 (8)–2.323 (8) Å). This difference could reflect rehybridization of platinum orbitals, due to the higher coordination number of Pt(1), or it could arise from steric congestion around Pt(1). The Pt(1)–P(7) distance (2.293 (8) Å) is with the range of Pt–P bond lengths in phosphite complexes.[18]

The carbonyl ligand adopts a distorted, triply bridging geometry, binding more strongly to Pt(1) than to Pt(2) or Pt(3). This is apparent from the respective Pt–C distances (1.93 (3), 2.16 (3), and 2.27 (3) Å) and from the Pt(1)–C–O bond angle (155 (2)°), which is significantly larger than the Pt(2)–C–O and Pt(3)–C–O angles (121 (2) and 120 (2)°). It is interesting to compare the geometry of the $Pt_3(\mu_3\text{-}CO)$ unit in 2c with those previously observed in the complexes $[Pt_3(\mu_3\text{-}CO)(\mu\text{-dppm})_3]^{2+}$ (1), $[Pt_3(\mu_3\text{-}CO)(\mu_3\text{-}SnF_3)(\mu\text{-dppm})_3]^+$ (3), and $[Pt_3(\mu_3\text{-}CO)(SCN)(\mu\text{-dppm})_3]^+$. A brief summary provided in Table II, where the μ-dppm ligands are omitted for clarity, shows that the Pt–Pt distances are very similar for the 42e cluster 1, the 44e cluster with an additional triply bridging ligand 3, and the 44e clusters with an additional terminal ligand 4 and 2c. However, the distortion of the triply bridging carbonyl ligand from the symmetrical μ_3-bonding mode is significant in the weakly bound thiocyanate adduct 4, and it is even greater in the more strongly bound triphenyl phosphite adduct 2c. This distortion will be considered further in the Discussion.

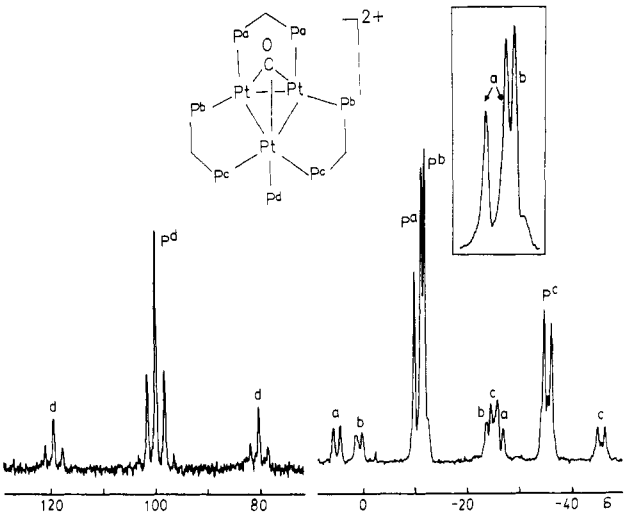

Figure 3. ^{31}P NMR spectrum (121.5 MHz) of **2a** at −92 °C.

Characterization of Complexes 2a–f by Spectroscopic Methods. The values for the ν(CO) stretching frequencies were in the narrow range 1774–1780 cm^{-1} for the stable clusters **2a–d**. This is in the range of stretching frequencies for μ_3-CO groups but is higher than ν(CO) = 1765 cm^{-1} for the parent cluster 1. We note that complex 3, with a symmetrical $Pt_3(\mu_3\text{-}CO)$ group, has a still higher value of ν(CO) = 1827 cm^{-1}, and it is therefore possible that the higher ν(CO) values are characteristics of 44e clusters and are not primarily dependent on whether the $Pt_3(\mu_3\text{-}CO)$ group is symmetrical or not (Table II).

The complexes 2 were fluxional at room temperature, and so NMR spectra were obtained at low temperature, typically at −90 °C in acetone-d_6 solution. The ^1H NMR spectra in the CH_2P_2 region (Table III) contained two "AB" quartets with relative areas 2:1 as expected for the static structure 2, which has no plane of symmetry containing the $Pt_3(PCP)_3$ unit.

The ^{31}P NMR spectra of the complexes are informative, and the spectrum of **2a** (Figure 3) will be described as a typical example. Data for all complexes are given in Table IV. In these $Pt_3(\mu\text{-dppm})_3$ complexes, the largest J(PP) couplings are the translike couplings through the Pt–Pt bonds, which in 2 are $^3J(P^aP^c)$ and $^3J(P^bP^{b\prime})$. The spectra contain two doublet resonances and singlet resonance, and the singlet is then readily assigned to P^b. The magnitude of $^3J(P^bP^{b\prime}) = 150$ Hz, obtained from the ^{195}Pt satellite spectra, while $^3J(P^aP^c) = 170$ Hz, and these are typical values for complexes 2 (Table IV). The resonances due to P^a ($\delta = -10.8$, $^1J(PtP) = 3930$ Hz) and P^c ($\delta = -35.6$, $^1J(PtP) = 2500$ Hz) are assigned by correlation of $^1J(PtP)$ values with the Pt–P bond distances (Pt–P^c longer than

(17) Ling, S. S. M.; Hadj-Bagheri, N.; Manojlović-Muir, Lj.; Muir, K. W.; Puddephatt, R. J. *Inorg. Chem.* **1987**, *26*, 231.
(18) Bao, Q.-B.; Geib, S. J.; Rheingold, A. L.; Brill, T. B. *Inorg. Chem.* **1987**, *26*, 3453.

Table III. ^{1}H NMR Data (−80 °C) for Complexes 2a–d in Acetone-d_6

	$P_2CH^aH^b$			$P_2CH^cH^d$				
complex[a]	δ_a	δ_b	$^2J_{H^aH^b}$/Hz	δ_c	δ_d	$^2J_{H^cH^d}$/Hz	δ_e	J_{PH}/Hz
2a	4.91	4.86	14	5.93	5.88	14	3.51	10.8
2b	4.46			5.69	5.55	14	4.30	7
2c	4.92	4.80	14	5.75	5.62	14		
2d							1.64	13

[a] Legend: **2a**, $P(OCH_3^e)_3$; **2b**, $P(OCH_2^eCH_3^f)_3$, δ_f = 1.3, t, $^3J(H^eH^f)$ = 7 Hz; **2c**, $P(OC_6H_5)_3$; **2d**, $P(CH_3^e)_2C_6H_5$, spectrum very poorly resolved in the CH_2 region and assignments are not given.

Table IV. ^{31}P NMR Data (−92 °C) for the Clusters 2a–f

complex	2a	2b	2c	2d	2e	2f	
$\delta(P^a)$	−10.8	−10.0	−12.4	−13.9	−16.1	−15.4	−5.1[b]
$^1J(PtP^a)$	3930	3820	3930	3820	3800	3860	3860
$^3J(P^aP^c)$	170	180	170	170	170	170	170
$\delta(P^b)$	−12.1	−14.6	−13.6	−13.6	−15.3	−7.9	
$^1J(PtP^b)$	3080	3060	3000	3080	3100	2780	
$^3J(P^bP^{b'})$	150	150	150	150	160		
$\delta(P^c)$	−35.6	−37.9	−35.7	−42.4	−42.5	−43.1	−38.7[b]
$^1J(PtP^c)$	2500	2400	2665	2640	2600	2660	2660
$^3J(P^aP^c)$	170	180	170	170	170	170	170
$\delta(P^d)$	100.3	97.8	91.9	−35.6	−18.8	−7.0	
$^1J(Pt^1P^d)$	4910	4990	5080	2800	2750	2670	
$^2J(Pt^2P^d)$	420	410	430	186	240	220	

[a] All J values are in Hz. [b] Complex **2f** gives two P^a and P^c resonances; see text.

Table V. ^{13}C NMR Data for Complexes 2 in CD_2Cl_2

	2a	2c	2g
δ(CO)/ppm	194.5	194.0	194.0
$^1J(Pt^1C)$/Hz	996	960	
$^1J(Pt^2C)$/Hz	468	463	
$J_{av}(PtC)$[a]/Hz	630[b]	630[c]	640
$^2J(P^dC)$/Hz	142	146	144

[a] Experimental value in region of rapid fluxionality. [b] Calculated value $J_{av}(PtC) = (^1/_3 \times 996) + (^2/_3 \times 468) = 644$ Hz. [c] Calculated value $J_{av}(PtC) = (^1/_3 \times 960) + (^2/_3 \times 463) = 629$ Hz.

Pt–P^a, Table I) and from a general trend that the ^{31}P chemical shifts are more negative when bound to platinum atoms with higher steric hindrance.[17]

The resonance due to the $P(OMe)_3$ ligand was at δ = 100.3 and appeared as a 1:4:1 triplet (due to coupling to Pt^1, $^1J(PtP)$ = 4910 Hz) of 1:8:18:8:1 quintets (due to coupling to Pt^2 and Pt^3, $^2J(PtP)$ = 420 Hz). These parameters were typical for the phosphite adducts, but lower $J(PtP)$ values were found for the phosphine complexes as seen in Table IV.

The ^{13}C NMR spectrum of **2a***, enriched with ^{13}CO, gave $\delta(^{13}CO)$ = 194.5 ppm, which appeared as a 1:1 doublet (coupling to $P(OMe)_3$, $^2J(PC)$ = 142 Hz) of 1:4:1 triplets (due to coupling to Pt^1, $^1J(PtC)$ = 996 Hz) of 1:8:18:8:1 quintets (due to coupling to Pt^2 and Pt^3, $^1J(PtC)$ = 468 Hz). The data are in Table V.

The above spectroscopic data clearly show that the structures in solution are of the type found in the solid state for **2c**. In particular, the phosphine or phosphite ligands adopt a terminal bonding position and the carbonyl group is asymmetrically bridging with a much stronger interaction with Pt^1 than with Pt^2 or Pt^3.

For the bulky PPh_3 derivative **2f**, the ^{31}P NMR spectrum at −90 °C showed a doubling of some of the resonances and data are given in Table IV. It is not clear if the extreme steric hindrance expected for this species causes nonequivalence of pairs of atoms, $P^aP^{a'}$ and $P^cP^{c'}$, within a given molecule or if two atropisomers are formed.[19]

(19) Blau, R. J.; Espenson, J. H.; Kim, S.; Jacobson, R. A. *Inorg. Chem.* **1986**, *25*, 757.

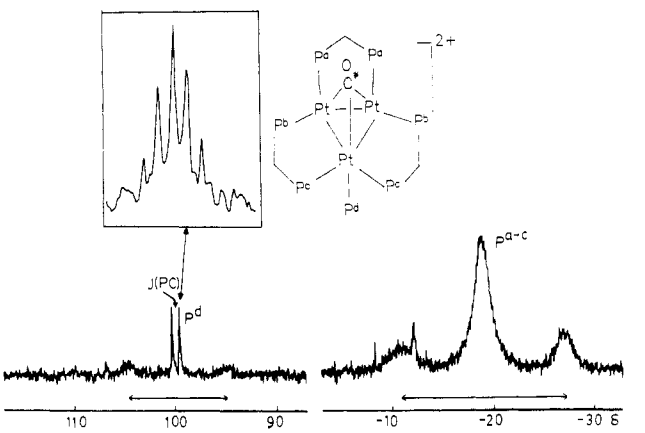

Figure 4. ^{31}P NMR spectrum (121.5 MHz) of **2a*** (^{13}CO labeled) at 60 °C. The expansion shows one of the peaks due to the $P(OMe)_3$ phosphorus, illustrating the septet structure due to coupling to six dppm ^{31}P atoms.

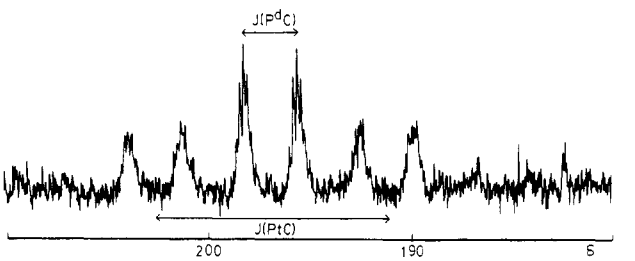

Figure 5. ^{13}C NMR spectrum (75.6 MHz) of **2a*** at 60 °C.

The former is perhaps more probable since only one signal due to coordinated PPh_3 was resolved.

Fluxionality of Complexes 2a–f. The clusters **2a–e** were found to be fluxional in the sense that the ligand L could migrate around the triangular face of the cluster **2** as shown in eq 1.

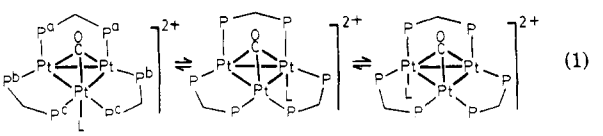
(1)

For **2a** and **2a***, which were studied in the most detail, the ^{31}P NMR spectrum at 60 °C (Figure 4) showed a single broad resonance due to the dppm phosphorus atoms, thus indicating apparent 3-fold symmetry for the complex. The resonance due to the $P(OMe)_3$ ligand occurred as a sharp septet due to coupling to six "equivalent" dppm phosphorus atoms and had broad satellites due to $^1J(PtP)$ = 1900 Hz. The calculated value for rapid intramolecular fluxionality (eq 1) would be $^1J(PtP)' = (^1/_3 \times 4910) + (^2/_3 \times 420) = 1917$ Hz, in reasonable agreement. A diagram of the spectra has been published.[15] The ^{195}Pt satellites were sharper at 100 °C in DMF solution with $^1J(PtP)$ = 1910 Hz, but the complex began to decompose under these conditions. Finally, in the presence of free $P(OMe)_3$, no exchange between free and coordinated $P(OMe)_3$ could be detected by NMR spectroscopy at 60 °C in acetone, indicating that the exchange process did not involve reversible dissociation of $P(OMe)_3$. This was confirmed by the observation of coupling between the $P(OMe)_3$ phosphorus and ^{13}CO in **2a** (Figure 4).

Further evidence on the nature of the fluxionality was obtained by ^{13}C NMR spectroscopy of **2a** and **2c**. At 60 °C the ^{13}CO resonance in each case still occurred as a doublet with $^2J(PC)$ = 144 Hz, due to coupling to the phosphite phosphorus, but an average ^{195}Pt coupling of $^1J(PtC)$ = 630 Hz was observed (Figure 3). The calculated average value of $^1J(PtC) = (^1/_3 \times 996) + (^2/_3 \times 468) = 644$ Hz. Thus, the carbonyl appears to be symmetrically triply bridging in the fast-fluxionality region but the coupling $^2J(PC)$ to the phosphite ligand is maintained. This confirms that the fluxionality does not involve reversible dissociation of either the phosphite or carbonyl ligand and so supports the mechanism of eq 1. A transition state with a $Pt_3(\mu_3\text{-}PX_3)$ group and *symmetrical* $Pt_3(\mu_3\text{-}CO)$ group is probable but not proved.[20]

The results described above are in sharp contrast with those obtained for the triphenylphosphine adduct **2f**. For this complex at −43 °C, sharp singlet resonances due to dppm and PPh_3 phosphorus atoms were observed, the latter having no ^{195}Pt satellites. The chemical shifts were close to those for free **1** and PPh_3. At this temperature the equilibrium strongly favors **1** and PPh_3 over **2f**, but it is probable that there is fast exchange also. As discussed earlier, the steric bulk of PPh_3 appears to be at the limit for access to the Pt_3 plane of **1**. It is not clear if the intramolecular migration of eq 1 can occur in this case, since the complex is almost completely dissociated at temperatures where it might occur.

The fluxionality observed for **2a–e** appears to be unique in cluster complexes and is probably due to a small energy difference between the structures with terminal and μ_3-PR_3 ligands. Phosphine or phosphite fluxionality in transition-metal clusters has previously been considered not to occur.[21-23] The related fluxionality of a diphosphine ligand has recently been reported.[24-26]

Spectroscopic Characterization of $[Pt_3(\mu_3\text{-}CO)(\mu\text{-dppm})_3(PF_3)]^{2+}$. On the basis of the above studies of fluxionality, it seemed that the most probable ligand to form a complex with a $Pt_3(\mu_3\text{-}PX_3)$ group was PF_3, which has π-acceptor properties similar to those of CO. An isolobal analogy also exists between PF_3 and $[SnF_3]^-$, which forms the symmetrical $Pt_3(\mu_3\text{-}SnF_3)$ group in **3**, and this also suggested that the PF_3 adduct might have structure **5** rather than **2g**.

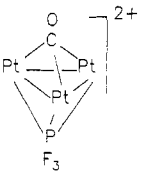

5

The PF_3 adduct must be characterized in solution in the presence of some free PF_3, since partial dissociation occurs on attempted isolation. Even at −92 °C, in CD_2Cl_2 solution, the ^{31}P NMR spectrum contained only one resonance due to the μ-dppm ligands (Table III) at δ = −17.7 ($^1J(PtP)$ = 3370 Hz), while the PF_3 signal occurred as a broad, poorly resolved quartet at δ = −15.9 ($^1J(PF)$ = 1440 Hz). In the ^{13}C NMR spectrum at −92 °C, the carbonyl resonance was at δ = 194.0 as a 1:1 doublet ($^2J(F_3PCO)$ = 144 Hz) of 1:12:49:84:49:12:1 septets (due to coupling to three "equivalent" platinum atoms, $^1J(PtC)$ = 640 Hz).

There are strong similarities between the above spectra and those due to the complexes **2a** and **2b** in the high-temperature limiting spectra where phosphite fluxionality is rapid, but there is also a strong resemblance to the spectrum of **3**, which contains a symmetrical μ_3-SnF_3^- ligand. Thus, the PF_3 adduct either has structure **2g** but is still undergoing rapid intramolecular fluxionality of the PF_3 ligand even at −92 °C or it has the structure **5**. In either case, the prediction that PF_3 would have a stronger tendency than the phosphite or phosphine ligands to form the $Pt_3(\mu_3\text{-}PX_3)$ group is clearly confirmed. Attempts to grow crystals of **2g** or **5** suitable for X-ray structure determination have so far been unsuccessful.

Discussion

This work has shown (i) that phosphine and phosphite ligands add to complex **1** as terminal ligands and (ii) that this ligand addition leads to a slippage of the μ_3-carbonyl ligand *toward* the platinum atom with the highest coordination number in complexes **2**. This observation can be rationalized if the μ_3-CO ligand acts to a large extent as a π-acceptor ligand,[7,17] and this interpretation has been expressed elegantly by Evans.[10] According to extended Hückel MO calculations (EHMO), the platinum acceptor orbital is a $5d_{z^2}6p_z$ hybrid orbital and the enhanced back-bonding can then be understood in terms of the bonding interactions.

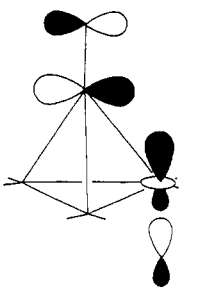

While this interaction might be expected to lead to a lower value of ν(CO) in **2** compared to that in **1**, the opposite effect was observed (Table II). One possible reason for this is that the geometry of the $Pt_3(\mu_3\text{-}CO)$ unit changes from an almost regular triply bridging mode in **1** to that

(20) A transition state with a μ_2-PR_3 group is also possible but is considered less likely because steric hindrance would be greater.
(21) Farrar, D. H.; Lunniss, J. A. *J. Chem. Soc., Dalton Trans.* **1987**, 1249.
(22) Alex, R. F.; Pomeroy, R. K. *Organometallics* **1987**, *6*, 2437.
(23) Shaffer, M. R.; Keister, J. B. *Organometallics* **1986**, *5*, 561.
(24) Sutin, K. A.; Kolis, J. W.; Mlekuz, M.; Bougeard, P.; Sayer, B. G.; Quilliam, M. A.; Faggiani, R.; Lock, C. J. L.; McGlinchey, M. J.; Jaouen, G. *Organometallics* **1987**, *6*, 439.
(25) Dean, P. A. W.; Vittal, J. J.; Srivastava, R. S. *Can. J. Chem.* **1987**, *65*, 2628.
(26) Bradford, A. M.; Puddephatt, R. J. *New J. Chem.* **1988**, *12*, 427.

which may be regarded as a semibridging mode in **2c** (Table II). This is not just a solid-state effect, since the low-temperature ^{13}C NMR spectrum in the carbonyl region of **2a** shows a much larger coupling to Pt^1 ($^1J(Pt^1C)$ = 996 Hz) than to Pt^2 and Pt^3 ($^1J(Pt^2C) = {}^1J(Pt^3C)$ = 468 Hz). The geometry of the $Pt_3(\mu_3\text{-CO})$ unit is then intermediate between that expected for a symmetrical μ_3-CO group and that expected for a terminal carbonyl bond to Pt^1, and the slight increase in ν(CO) for **2** compared to the value for **1** is not unreasonable on that basis.

Evans has suggested,[10] on the basis of EHMO calculations, that the symmetrical structure $[Pt_3(\mu_3\text{-CO})_2(\mu\text{-dppm})_3]^{2+}$ (**6**) is slightly more stable than the structure of $[Pt_3(\mu_3\text{-CO})(CO)(\mu\text{-dppm})_3]^{2+}$ (**7**), analogous to the case for **2**. The symmetrical structure was also consistent with the NMR data, but the observation of a terminal carbonyl stretching band in the IR spectrum indicated that **7** was the correct structure but that it was fluxional even at −90 °C. There are now good examples, **3** and **2c**, for which the added ligand is clearly in a μ_3-bridging site and a terminal site, respectively, and so the spectroscopic properties of each type of complex are not established (Table II). Unfortunately, the IR and NMR parameters are very similar for **3** and for **2a** in the rapid-fluxionality region. Thus, for the PF_3 complex it is not possible to distinguish between structure **5** or a rapidly fluxional **2g**. The similarities of the bonding properties of CO and PF_3 are well-known, and so it is not unreasonable that **2g** and **5** are very similar in energy, as are **6** and **7**. However, there are no known examples of bridging PX_3 ligands, and so the possibility that **5** is the correct structure is particularly intriguing. For rapid fluxionality of **2g** at −90 °C, $\Delta G^{\ddagger}$ is probably ≤40 kJ mol^{-1}, and this may be considered an upper limit of the thermodynamic preference for **2g** over **5**. While the structure **2g** is perhaps more probable than **5**, this work does show the feasibility of synthesis of a $Pt_3(\mu_3\text{-}PF_3)$ group and hence other $M_3(\mu_3\text{-}PF_3)$ groups.

Experimental Section

IR spectra were recorded as Nujol mulls by using a Bruker IFS/32 FTIR spectrometer. ^1H NMR spectra were recorded by using a Varian XL-200 spectrometer, while $^{13}C\{^1H\}$, $^{31}P\{^1H\}$, and $^{195}Pt\{^1H\}$ NMR spectra were recorded by using a Varian XL-300 spectrometer. References used were Me_4Si (^1H, ^{13}C), H_3PO_4 (^{31}P), and aqueous $K_2[PtCl_4]$ (^{195}Pt). The complex $[Pt_3(\mu_3\text{-CO})(\mu\text{-dppm})_3][PF_6]_2$ (**1**[PF_6]$_2$) was prepared as described previously.[2] Elemental analyses were performed by Guelph Chemical Laboratories.

$[Pt_3(\mu_3\text{-CO})(\mu\text{-dppm})_3(P(OMe)_3)][PF_6]_2$ (2a[PF_6]$_2$). To a solution of complex **1** (40 mg) in acetone (10 mL) was added $P(OMe)_3$ (2.29 μL) by syringe. The solvent was evaporated under vacuum to give the product **2a**, which could be crystallized from acetone/pentane or CH_2Cl_2/pentane as orange crystals. The reaction was essentially quantitative as monitored by ^{31}P NMR spectroscopy, and isolated yields were ~80%. Anal. Calcd for $C_{79}H_{75}F_{12}O_4P_9Pt_3$: C, 43.5; H, 3.5. Found: C, 43.2; H, 3.5. IR: ν(CO) = 1780 cm^{-1}.

The following complexes were similarly prepared. Anal. Calcd for $[Pt_3(\mu_3\text{-CO})(\mu\text{-dppm})_3(P(OEt)_3)][PF_6]_2$ (**2b**[PF_6]$_2$), $C_{82}H_{81}F_{12}O_4P_9Pt_3$: C, 44.3; H, 3.7. Found: C, 44.4; H, 3.9. IR: ν(CO) = 1779 cm^{-1}. Anal. Calcd for $[Pt_3(\mu_3\text{-CO})(\mu\text{-dppm})_3(P(OPh)_3)][PF_6]_2$ (**2c**[PF_6]$_2$, $C_{94}H_{81}F_{12}O_4P_9Pt_3$: C, 47.7; H, 3.5. Found: C, 45.8; H, 3.7 (poor analysis due to occluded solvent, see later). IR: ν(CO) = 1779 cm^{-1}. Anal. Calcd for $[Pt_3(\mu_3\text{-CO})(\mu\text{-dppm})_3(PMe_2Ph)][PF_6]_2$ (**2d**[PF_6]$_2$) $C_{84}H_{77}F_{12}OP_9Pt_3$: C, 46.0; H, 3.5. Found: C, 46.4; H, 4.0. IR: ν(CO) = 1774 cm^{-1}.

Equilibrium Constant for Formation of $[Pt_3(\mu_3\text{-CO})(\mu\text{-dppm})_3(PPh_3)][PF_6]_2$ (2f[PF_6]$_2$). To a solution of **1** (40 mg) in acetone-d_6 (0.50 mL) in an NMR tube was added PPh_3 (5.1 mg). Integration of ^{31}P NMR signals due to free and coordinated PPh_3 NMR singals due to free and coordinated PPh_3 and free **1** allowed the equilibrium constant to be determined over the range −83 to −92 °C. At higher temperatures, the signals were too broad to be useful. Typical values of K/L mol^{-1} are 7.8 at 190 K, 22.4 at 183 K, and 28.6 at 181 K.

$[Pt_3(\mu_3\text{-CO})(\mu\text{-dppm})_3(PF_3)][PF_6]_2$ (2g[PF_6]$_2$). Excess PF_3 was added to an NMR tube, fitted with a Teflon tap, containing a solution of complex **1** (40 mg) in CD_2Cl_2 (0.5 mL) at liquid-N_2 temperature. The tube was sealed, warmed to −78 °C, and shaken to mix thoroughly. Most of the excess PF_3 was then removed by pumping at −78 °C; the tube was sealed again, and NMR spectra were recorded.

When the solvent was evaporated from such solutions, a mixture of **2g** and **1** was obtained, as shown by ^{31}P NMR spectroscopy.

X-ray Crystal Structure Analysis of $[Pt_3(\mu_3\text{-CO})(\mu\text{-dppm})_3(P(OPh)_3)]_2$ (2c[PF_6]$_2$). Red crystals of **2c** were obtained from an acetone solution. A crystal was sealed in a capillary and mounted on an Enraf-Nonius CAD4 diffractometer. All X-ray measurements were made with graphic-monochromated molybdenum radiation.

The unit cell constants (Table VI) were determined by a least-squares treatment of 23 reflections with $8 \le \theta \le 12°$. Preliminary investigation of the difraction pattern revealed a primitive crystal lattice and the $2/m$ Laue symmetry. The systematic absences of reflections were compatible with the space group $P2_1/c$.

Intensities of 11 869 reflections with $4 \le 2\theta \le 42°$ were measured by continuous $\theta/2\theta$ scans. The scan widths in θ were 0.80°, and the scan speeds were adjusted to give $\sigma(I)/I \le 0.02$, subject to the time limit of 120x. Two strong reflections were remeasured every 2 h, but their intensities showed only random fluctuations, not exceeding 4% at the mean values. The integrated intensities, derived in the usual manner,[27] were corrected for Lorentz, polarization, and absorption effects. The absorption correction was made by the empirical method of Walker and Stuart.[28] A total of 3987 symmetry-related reflections were averaged to yield 1958 independent ones and R values (internal) of 0.075 before, and 0.050 after, absorption correction. Only 3967 unique reflections for which $I \ge 3\sigma(I)$ were used in the structure analysis.

The crystal structure was determined by the heavy-atom method. The positions of the metal atoms were obtained from a Patterson function and those of the remaining non-hydrogen atoms from difference electron density maps. The structure was

Table VI. Crystallographic Data for $[Pt_3(\mu_3\text{-CO})(\mu\text{-dppm})_3(P(OPh)_3)][PF_6]_2$ (2c[PF_6]$_2$)[a]

formula	$C_{94}H_{81}F_{12}O_4P_9Pt_3$
space group	$P2_1/c$
a/Å	19.239 (6)
b/Å	19.461 (10)
c/Å	26.137 (10)
β/deg	110.28 (3)
v/Å^3	9179 (7)
Z	4
F_{000}	4616
d_{calc}/g cm^{-3}	1.713
cryst dimens/mm	0.36 × 0.24 × 0.16
temp °C	23
radiation (wavelength/Å)	Mo Kα (0.710 69)
μ(Mo Kα)/cm^{-1}	48.4
data collecn range (2θ)/deg	4–42
abs factors (on F)	0.81–1.17
no. of unique rflns with $I \ge 3\sigma(I)$	3967
no. of params refined	351
R[b]	0.0475
R_w[c]	0.0545
largest param shift/esd (final cycle)	0.09
largest peak in final ΔF map/e Å^{-3}	1.3

[a] The data in this table make no allowance for unidentified solvent molecules. [b] $R = \sum||F_o| - |F_c||/|F_o|$. [c] $R_w = [\sum w(|F_o| - |F_c|)^2/\sum w|F_o|^2]^{1/2}$, $w = 1/\sigma^2(|F_o|)$.

(27) Manojlović-Muir, Lj.; Muir, K. W. *J. Chem. Soc., Dalton Trans.* **1974**, 2427.
(28) Walker, N.; Stuart, D. *Acta Crystallogr., Sect. A: Found. Crystallogr.* **1986**, *A39*, 158.

Table VII. Fractional Atomic Coordinates and Thermal Parameters for $[Pt_3(\mu_3\text{-}CO)(\mu\text{-dppm})_3(P(OPh)_3)][PF_6]_2$ (2c$[PF_6]_2$)

atom	x	y	z	U^a/Å^2	atom	x	y	z	U^a/Å^2
Pt(1)	−0.24987 (7)	0.12158 (6)	0.28551 (4)	0.027	C(C2)	−0.4443 (14)	0.2740 (14)	0.0637 (5)	0.067 (10)
Pt(2)	−0.25422 (7)	0.13492 (6)	0.18332 (4)	0.029	C(C3)	−0.5134 (10)	0.2743 (13)	0.0234 (10)	0.067 (10)
Pt(3)	−0.16941 (7)	0.04082 (6)	0.24780 (4)	0.029	C(C4)	−0.5653 (15)	0.2255 (20)	0.0237 (10)	0.067 (10)
P(1)	−0.3194 (4)	0.2190 (4)	0.2892 (3)	0.036	C(C5)	−0.5481 (14)	0.1764 (14)	0.0643 (5)	0.078 (11)
P(2)	−0.3386 (4)	0.2251 (4)	0.1622 (3)	0.037	C(C6)	−0.4790 (10)	0.1761 (13)	0.1046 (10)	0.056 (9)
P(3)	−0.2249 (4)	0.1021 (4)	0.1091 (3)	0.035	C(D1)	−0.2941 (18)	0.3070 (14)	0.1591 (7)	0.041 (8)
P(4)	−0.1223 (4)	−0.0011 (4)	0.1848 (3)	0.037	C(D2)	−0.2243 (20)	0.3066 (12)	0.1554 (14)	0.47 (9)
P(5)	−0.1260 (4)	−0.0255 (4)	0.3253 (3)	0.037	C(D3)	−0.1865 (11)	0.3675 (18)	0.1580 (11)	0.078 (11)
P(6)	−0.1820 (4)	−0.0953 (4)	0.3764 (3)	0.034	C(D4)	−0.2185 (18)	0.4289 (14)	0.1644 (7)	0.077 (12)
P(7)	−0.3424 (4)	0.0409 (4)	0.2643 (3)	0.036	C(D5)	−0.2883 (20)	0.4293 (12)	0.1682 (14)	0.108 (15)
P(F1)	0.2041 (7)	0.3890 (7)	0.5347 (5)	0.174	C(D6)	−0.3261 (11)	0.3683 (18)	0.1655 (11)	0.077 (11)
P(F2)	−0.7078 (7)	0.1426 (8)	0.3778 (8)	0.324	C(E1)	−0.2987 (13)	0.1017 (17)	0.0411 (8)	0.031 (7)
O(1)	−0.3440 (10)	0.0058 (10)	0.3175 (7)	0.046 (6)	C(E2)	−0.3148 (12)	0.0454 (12)	0.0069 (12)	0.042 (8)
O(2)	−0.4200 (10)	0.0755 (9)	0.2366 (7)	0.039 (5)	C(E3)	−0.3703 (18)	0.0492 (11)	−0.0435 (10)	0.063 (10)
O(3)	−0.3423 (10)	−0.0278 (9)	0.2312 (7)	0.047 (5)	C(E4)	−0.4097 (13)	0.1094 (17)	−0.0597 (8)	0.050 (9)
O(4)	−0.1176 (11)	0.1904 (10)	0.2663 (7)	0.049 (6)	C(E5)	−0.3936 (12)	0.1657 (12)	−0.0255 (12)	0.058 (10)
F(11)	0.248 (2)	0.325 (2)	0.561 (2)	0.34 (3)	C(E6)	−0.3381 (18)	0.1619 (11)	0.0249 (10)	0.050 (9)
F(12)	0.161 (2)	0.453 (2)	0.508 (2)	0.31 (2)	C(F1)	−0.1509 (11)	0.1515 (13)	0.0957 (8)	0.041 (8)
F(13)	0.268 (3)	0.434 (3)	0.570 (1)	0.38 (3)	C(F2)	−0.1438 (20)	0.1465 (17)	0.0451 (6)	0.065 (10)
F(14)	0.140 (3)	0.344 (3)	0.500 (1)	0.44 (4)	C(F3)	−0.0873 (17)	0.1809 (11)	0.0348 (9)	0.068 (10)
F(15)	0.169 (2)	0.392 (1)	0.579 (1)	0.36 (3)	C(F4)	−0.0379 (11)	0.2203 (13)	0.0751 (8)	0.081 (12)
F(16)	0.239 (2)	0.386 (1)	0.490 (1)	0.26 (2)	C(F5)	−0.0451 (20)	0.2252 (17)	0.1257 (6)	0.075 (11)
F(21)	−0.689 (3)	0.103 (1)	0.334 (2)	0.54 (6)	C(F6)	−0.1016 (17)	0.1908 (11)	0.1360 (9)	0.065 (10)
F(22)	−0.727 (3)	0.182 (1)	0.422 (2)	0.79 (9)	C(G1)	−0.0384 (11)	0.0404 (15)	0.1821 (10)	0.038 (7)
F(23)	−0.694 (2)	0.211 (1)	0.354 (2)	0.43 (3)	C(G2)	−0.0169 (20)	0.0250 (17)	0.1382 (6)	0.050 (9)
F(24)	−0.721 (2)	0.075 (1)	0.402 (2)	0.27 (2)	C(G3)	0.0507 (17)	0.0474 (8)	0.1374 (11)	0.073 (10)
F(25)	−0.626 (2)	0.140 (4)	0.415 (2)	0.36 (3)	C(G4)	0.0969 (11)	0.0853 (15)	0.1805 (10)	0.087 (12)
F(26)	−0.789 (2)	0.145 (4)	0.341 (2)	0.39 (3)	C(G5)	0.0754 (20)	0.1007 (17)	0.2243 (6)	0.095 (13)
C(1)	−0.3746 (13)	0.2393 (12)	0.2194 (9)	0.025 (7)	C(G6)	0.0077 (17)	0.0783 (8)	0.2251 (11)	0.069 (10)
C(2)	−0.1950 (14)	0.0157 (13)	0.1159 (10)	0.031 (7)	C(H1)	−0.0981 (16)	−0.0912 (10)	0.1843 (14)	0.033 (7)
C(3)	−0.1607 (15)	0.0038 (14)	0.3786 (10)	0.039 (8)	C(H2)	−0.1398 (12)	−0.1381 (19)	0.1465 (11)	0.060 (9)
C(4)	−0.1715 (16)	0.1558 (14)	0.2621 (10)	0.038 (8)	C(H3)	−0.1177 (19)	−0.2059 (16)	0.1495 (7)	0.101 (14)
C(11)	−0.3770 (16)	−0.0553 (12)	0.3255 (8)	0.039 (8)	C(H4)	−0.0538 (16)	−0.2268 (10)	0.1903 (14)	0.055 (9)
C(12)	−0.3498 (13)	−0.1185 (16)	0.3177 (12)	0.061 (10)	C(H5)	−0.0121 (12)	−0.1798 (19)	0.2281 (11)	0.066 (10)
C(13)	−0.3789 (21)	−0.1778 (12)	0.3311 (15)	0.076 (11)	C(H6)	−0.0342 (19)	−0.1121 (16)	0.2251 (7)	0.056 (9)
C(14)	−0.4353 (16)	−0.1739 (12)	0.3523 (8)	0.113 (15)	C(I1)	−0.0251 (14)	−0.0209 (20)	0.3585 (9)	0.038 (8)
C(15)	−0.4625 (13)	−0.1107 (16)	0.3601 (12)	0.152 (19)	C(I2)	0.0154 (15)	−0.0722 (11)	0.3923 (7)	0.063 (10)
C(16)	−0.4334 (21)	−0.0514 (12)	0.3467 (15)	0.093 (13)	C(I3)	0.0895 (11)	−0.0621 (16)	0.4219 (12)	0.061 (10)
C(21)	−0.4933 (14)	0.0486 (22)	0.2264 (10)	0.052 (9)	C(I4)	0.1231 (14)	−0.0008 (20)	0.4178 (9)	0.093 (13)
C(22)	−0.5404 (24)	0.0941 (15)	0.2384 (10)	0.107 (14)	C(I5)	0.0827 (15)	0.0505 (11)	0.3840 (7)	0.73 (11)
C(23)	−0.6118 (21)	0.0743 (16)	0.2322 (16)	0.112 (15)	C(I6)	0.0086 (11)	0.0404 (16)	0.3544 (12)	0.053 (9)
C(24)	−0.6360 (14)	0.0091 (22)	0.2138 (10)	0.131 (17)	C(J1)	−0.1525 (17)	−0.1158 (11)	0.3209 (11)	0.028 (7)
C(25)	−0.5889 (24)	−0.0364 (15)	0.2018 (10)	0.104 (14)	C(J2)	−0.1478 (20)	−0.1526 (16)	0.3672 (9)	0.090 (13)
C(26)	−0.5175 (21)	−0.0166 (16)	0.2080 (16)	0.060 (10)	C(J3)	−0.1701 (10)	−0.2204 (13)	0.3628 (8)	0.093 (13)
C(31)	−0.3567 (16)	−0.0389 (15)	0.1769 (7)	0.030 (7)	C(J4)	−0.1971 (17)	−0.2514 (11)	0.3122 (11)	0.095 (13)
C(32)	−0.3453 (9)	−0.1045 (15)	0.1613 (11)	0.053 (9)	C(J5)	−0.2017 (20)	−0.2146 (16)	0.2660 (9)	0.084 (12)
C(33)	−0.3658 (18)	−0.1207 (7)	0.1067 (13)	0.076 (11)	C(J6)	−0.1794 (10)	−0.1468 (13)	0.2704 (8)	0.065 (10)
C(34)	−0.3977 (16)	−0.0714 (15)	0.0677 (7)	0.074 (11)	C(K1)	−0.0943 (16)	0.1410 (18)	0.4084 (6)	0.049 (8)
C(35)	−0.4091 (9)	−0.0058 (15)	0.0833 (11)	0.061 (10)	C(K2)	−0.857 (11)	0.2064 (19)	0.3911 (11)	0.047 (8)
C(36)	−0.3886 (18)	0.0104 (7)	0.1379 (13)	0.056 (10)	C(K3)	−0.0217 (14)	0.2428 (8)	0.4173 (10)	0.073 (11)
C(A1)	−0.3922 (11)	0.2186 (11)	0.3175 (10)	0.031 (7)	C(K4)	0.0337 (16)	0.2139 (18)	0.4607 (6)	0.084 (12)
C(A2)	−0.3944 (12)	0.1659 (13)	0.3522 (13)	0.041 (8)	C(K5)	0.0251 (11)	0.1484 (19)	0.4780 (11)	0.066 (10)
C(A3)	−0.4510 (9)	0.1631 (9)	0.3733 (7)	0.056 (9)	C(K6)	−0.389 (14)	0.1120 (8)	0.4518 (10)	0.074 (11)
C(A4)	−0.5052 (11)	0.2131 (11)	0.3597 (10)	0.061 (10)	C(L1)	−0.2229 (14)	0.1061 (7)	0.4304 (10)	0.037 (8)
C(A5)	−0.5030 (12)	0.2658 (13)	0.3249 (13)	0.51 (9)	C(L2)	−0.2603 (18)	0.0533 (10)	0.4447 (11)	0.045 (8)
C(A6)	−0.4464 (9)	0.2685 (9)	0.3038 (7)	0.056 (9)	C(L3)	−0.2926 (11)	0.0638 (10)	0.4837 (6)	0.055 (9)
C(B1)	−0.2659 (16)	0.2955 (13)	0.3197 (7)	0.030 (7)	C(L4)	−0.2874 (14)	0.1272 (7)	0.5084 (10)	0.072 (10)
C(B2)	−0.2747 (8)	0.3256 (10)	0.3649 (8)	0.041 (8)	C(L5)	−0.2499 (18)	0.1801 (10)	0.4941 (11)	0.087 (12)
C(B3)	−0.2328 (17)	0.3822 (9)	0.3887 (10)	0.048 (8)	C(L6)	−0.2177 (11)	0.1696 (10)	0.4551 (6)	0.063 (10)
C(B4)	−0.1820 (16)	0.4087 (13)	0.3674 (7)	0.056 (9)	O(S)[b]	0.2324 (20)	0.1313 (20)	0.5260 (14)	0.203 (16)
C(B5)	−0.1732 (8)	0.3786 (10)	0.3223 (8)	0.070 (10)	C(S1)[b]	−0.518 (4)	−0.037 (4)	−0.493 (4)	0.24 (4)
C(B6)	−0.2151 (17)	0.3219 (9)	0.2984 (10)	0.047 (9)	C(S2)[b]	−0.477 (4)	0.001 (5)	−0.458 (3)	0.23 (3)
C(C1)	−0.4271 (15)	0.2249 (20)	0.1043 (10)	0.046 (8)					

[a] For oxygen, fluorine, and carbon atoms U is the refined isotropic thermal parameter. For platinum and phosphorus atoms U is the equivalent isotropic thermal parameter, defined as one-third of the trace of the orthogonalized U_{ij} tensor. [b] Atoms O(S), C(S1), and C(S2) belong to solvent molecules.

refined by minimizing the function $w[|F_o| - |F_c|)^2$, with $w = \sigma^{-2}(|F_o|)$.

At a later stage of refinement difference electron density maps showed three peaks that indicated the presence of two well-separated and only partially revealed solvent molecules. These peaks were allocated to the O(S) atom of one and C(S1) and C(S2) atoms of the other solvent molecule (Table VII), and all three atoms were allowed isotropic thermal parameters. The hydrogen atoms were included in the structural model in calculated positions, with C–H = 0.96 Å and U(isotropic) fixed at 0.05 Å^2. The 15 phenyl rings were refined as regular hexagons with C–C = 1.38 Å and the two PF_6^- anions as regular octahedrons with P–F = 1.53 Å; their carbon and fluorine atoms were refined with isotropic thermal parameters. Only the platinum and phosphorus atoms were allowed anisotropic thermal parameters. The refinement converged at $R = 0.0475$ and $R_W = 0.0545$. In the final difference electron density map the function values ranged from −1.1 to +1.3 e Å^{-3}, the extreme ones being associated with the positions of the

metal atoms and solvent molecules. The final atomic coordinates are shown in Table VII.

All calculations were performed on a GOULD SEL 32/37 computer, using the GX program package.[29] Neutral-atom scattering factors were taken from ref. 30.

(29) Mallinson, P. R.; Muir, K. W. *J. Appl. Crystallogr.* **1985**, *18*, 51.
(30) *International Tables for X-ray Crystallography*; Kynoch: Birmingham, England, 1974; Vol. IV, pp 99, 149.

Acknowledgment. We thank the NSERC (Canada) for financial support (to R.J.P.), the SERC (U.K.) for a research studentship (to G.D.), and NATO for a travel agent.

Supplementary Material Available: A table of anisotropic thermal parameters (1 page); a listing of observed and calculated structure amplitudes (20 pages). Ordering information is given on any current masthead page.

Syntheses of Organolanthanum and -cerium Cations and Labile Precursors

Paulette N. Hazin and Joseph W. Bruno*

Hall-Atwater Laboratories, Wesleyan University, Middletown, Connecticut 06457

Gayle K. Schulte

Chemical Instrumentation Center, Yale University, New Haven, Connecticut 06511

Received July 14, 1989

The lanthanide–iodide compounds $Cp''_2Ln(I)(NCMe)_2$ (Ln = La, Ce; Cp'' = 1,3-$C_5H_3(SiMe_3)_2$) serve as useful precursors for complexes containing the early-lanthanide fragments $[Cp''_2Ln^{III}]^+$. This moiety has been incorporated into compounds in which it binds either neutral or anionic ligands. Among these is the heterobimetallic compound $[Cp''_2Ce(\mu\text{-}\eta^2\text{-}OC)W(CO)(Cp)(\mu\text{-}\eta^2\text{-}CO)]_2$ (**3**), which is unusual in that the cerium(III) center is wholly nonemissive. This observation is explained on the basis of cerium-to-tungsten excited-state energy transfer, since dissolution in polar solvent (acetonitrile) leads to symmetrically solvated ions, loss of close Ce–W contact, and cerium(III) luminescence. Also, the cationic organolanthanide fragments have been seen to bind tetrafluoroborate anion, exhibiting an interesting trend in ligand lability; thus, in $Cp''_2Ln(NCMe)_2(FBF_3)$ (**4**), the nitrile ligands are more labile in THF solution than is the tetrafluoroborate ligand. Finally, the ionic compounds $[Cp''_2Ln(NCMe)(DME)][BPh_4]\cdot 0.5DME$ (**5**) have been prepared and the lanthanum analogue (**5b**) has been structurally characterized.

Introduction

Although the organometallic chemistry of the lanthanide elements has been developing rapidly for several years now,[1] it is apparent that much of this work has focused on the later lanthanides. The chemistry of these metals has proved diverse and interesting, and its development is facilitated by the variety of ligand spheres with which these smaller lanthanides can be stabilized. The earlier, larger lanthanides require a greater degree of steric saturation and have yet to exhibit many of the coordination spheres seen for later lanthanides. In spite of these apparent limitations, there are obvious reasons for pursuing early-lanthanide chemistry. Among the lanthanides, only cerium exhibits a stable +4 oxidation state.[2] While the oxidizing power of Ce(IV) is frequently utilized in organic syntheses,[3] this oxidation state has been observed in the stable organometallic compounds $(C_8H_8)_2Ce$ and $(Cp)_3Ce(O^iPr)$ (Cp = η^5-C_5H_5);[4] the former has been shown to be remarkably stable toward hydrolytic decomposition and is reduced to the trivalent anion $[(C_8H_8)_2Ce]^-$ only at very negative potentials.[4b] Also, the chemistries of trivalent lanthanum and cerium have been the subjects of several recent studies, in spite of the difficulties in achieving steric saturation. These efforts are in part spurred by the observation that the early lanthanides are very active catalysts for the polymerization of dienes and highly substituted olefins;[5] the catalysts are derived from mixtures of aluminum alkyls (e.g., $EtAlCl_2$) and either LnX_3 (X = Cl, Br)[5a] or $Ln(acac)_3$,[5b] and the most active catalysts contain Ce, Pr, or Nd. Additionally, $(Cp^*)_2LaCH(SiMe_3)_2$ and related derivatives (Cp* = η^5-C_5Me_5) constitute highly active catalysts or catalyst precursors in olefin hydrogenations, oligomerizations, and hydroamination systems.[6] This is significant since the lanthanides' terrestrial abundance percentages decrease in the order Ce > Nd > La > Gd, etc.[7]

(1) (a) Marks, T. J.; Ernst, R. D. In *Comprehensive Organometallic Chemistry*; Wilkinson, G., Stone, F. G. A., Abel, E. W., Eds.; Pergamon: Oxford, England, 1982; Chapter 21. (b) Schumann, H. *Angew. Chem., Int. Ed. Engl.* **1984**, *23*, 474–493. (c) Evans, W. J. *J. Organomet. Chem.* **1983**, *250*, 217–226. (d) Evans, W. J. *Polyhedron* **1987**, *6*, 803–835.
(2) Cotton, F. A.; Wilkinson, G. *Advanced Inorganic Chemistry*, 5th ed.; Wiley: New York, 1988; pp 975–977.
(3) (a) Fieser, L. F.; Fieser, M. *Reagents for Organic Synthesis*; Wiley: New York, 1967; pp 120–121. (b) Long, J. R. *Aldrichimica Acta* **1985**, *18*, 87–93.
(4) (a) Greco, A.; Cesca, S.; Bertolini, G. *J. Organomet. Chem.* **1976**, *113*, 321–330. (b) Streitwieser, A., Jr.; Kinsley, S. A.; Rigsbee, J. T.; Fragala, I. L.; Ciliberto, E.; Rosch, N. *J. Am. Chem. Soc.* **1985**, *107*, 7786–7788. (c) Gulino, A.; Casarin, M.; Conticello, V. P.; Gaudiello, J. G.; Mauermann, H.; Fragala, I.; Marks, T. J. *Organometallics* **1988**, *7*, 2360–2364. (d) Evans, W. J.; Deming, T. J.; Ziller, J. W. *Organometallics* **1989**, *8*, 1581–1582.
(5) (a) Rafikov, S. R.; Monakov, Yu. B.; Bieshev, Ya. Kh.; Valitova, I. F.; Murinov, Yu. I.; Tolstikov, G. A.; Nikitin, Yu. E. *Dokl. Akad. Nauk SSSR* **1976**, *229*, 1174–1176. (b) Fosong, W.; Renyu, S.; Yingtai, J.; Yuling, W.; Yulian, Z.; *Sci. Sin. (Engl. Ed.)* **1980**, *23*, 172–179. (c) Shen, Z. *Inorg. Chim. Acta* **1987**, *140*, 7–14. (d) Murinov, Yu. I.; Monakov, Yu. B. *Inorg. Chim. Acta* **1987**, *140*, 25–27. (e) Kozlov, V. G.; Marina, N. G.; Saval'eva, I. G.; Monakov, Yu. B.; Murinov, Yu. I.; Tolstikov, G. A. *Inorg. Chim. Acta* **1988**, *154*, 239–243. (f) Sabirov, Z. M.; Minchenkova, N. Kh.; Monakov, Yu. B. *Inorg. Chim. Acta* **1989**, *160*, 99–100.
(6) (a) Jeske, G.; Lauke, H.; Mauermann, H.; Swepston, P. N.; Schumann, H.; Marks, T. J. *J. Am. Chem. Soc.* **1985**, *107*, 8091–8103. (b) Jeske, G.; Schock, L. E.; Sweptson, P. N.; Schumann, H.; Marks, T. J. *J. Am. Chem. Soc.* **1985**, *107*, 8103–8110. (c) Jeske, G.; Lauke, H.; Mauermann, H.; Schumann, H.; Marks, T. J. *J. Am. Chem. Soc.* **1985**, *107*, 8111–8118. (d) Gagne, M. R.; Marks, T. J. *J. Am. Chem. Soc.* **1989**, *111*, 4108–4110.
(7) Huheey, J. *Inorganic Chemistry*, 3rd ed.; Harper and Row: New York, 1983; pp 912–913.

0276-7333/90/2309-0416$02.50/0